From these equations Weber (*15*) obtained

$$\tan \Delta = \omega \tau (r_0 - r_\infty)(2R\tau)/\{m(1 + \omega^2\tau^2) + (2R\tau/3)[2 + r_0 - r_\infty(4r_0 - 1)] + (2R\tau)^2(1 + 2r_\infty)(1 - r_\infty)\} \quad (7)$$

and

$$\tan \Delta_{max} = \omega \tau (r_0 - r_\infty)/\{1/3[(2 + r_0) - r_\infty(4r_0 - 1)] + 2[m(1 + 2r_\infty)(1 - r_\infty)(1 + \omega^2\tau^2)]^{1/2}\} \quad (8)$$

For $r_\infty = 0$, Eqs. 7 and 8 reduce to forms applicable to free isotropic rotations.

Since r_∞ is a measure of the degree to which the depolarizing rotations of DPH are restricted, we wished to use our measurements to obtain r_∞ in DMPC bilayers at various temperatures. Differential phase measurements alone do not yield r_∞. However, in a hindered environment both the steady-state anisotropy and the differential tangent are functions of r_∞ and R. With these measurements and the fluorescence lifetime it should be possible to determine r_∞ and R. By integrating and normalizing Eqs. 5 and 6 over times from 0 to infinity we obtained

$$r_\infty = r + \frac{(r - r_0)}{6R\tau} \quad (9)$$

Substituting Eq. 9 into Eq. 7 gives

$$(C \tan \Delta)(2R\tau)^2 + (D \tan \Delta - A)(2R\tau) + (E \tan \Delta - B) = 0 \quad (10)$$

where

$$A = 3B = \omega\tau(r_0 - r)$$
$$C = (1 + 2r)(1 - r)$$
$$D = 1/3(2r - 4r^2 + 2) \quad (11)$$
$$E = C/9 + m\omega^2\tau^2$$

By measuring tan Δ, r, and τ, one can obtain R from Eq. 10. This value of R may then be substituted into Eq. 9 to calculate r_∞. The values for r_∞ so obtained are presented in Fig. 4. It is apparent from these data that DPH is highly hindered at temperatures below the transition temperature of the bilayer ($r_\infty \simeq 0.3$) and that DPH rotates freely above the transition temperature ($r_\infty \simeq 0$). The midpoint of the change in r_∞ occurs at 24°C, which is near the phase transition temperature (*8*).

Using time-resolved decays of fluorescence anisotropy, Chen *et al.* (*10*) found $r_\infty \simeq 0.25$ below the transition temperature and $r_\infty \simeq 0.01$ above the transition temperature. Our results are in excellent agreement with those of Chen *et al.* However, the rapidity with which differential tangents may be measured allowed us to obtain a complete temperature profile for r_∞ (Fig. 4). Thus differential phase fluoreometry will be a powerful method for investigating hindered motions of fluorophores in lipid bilayers.

The detection of restricted diffusional motions of DPH in lipid bilayers illustrates the difficulties inherent in the extrapolation of DPH fluorescence anisotropy data to estimate membrane microviscosity. In such extrapolations it is assumed that the depolarizing rotations of DPH in the bilayers are identical to those in the reference solvent, which is usually a mixture of branched-chain alkanes. Our data demonstrate that this assumption is not valid, a result that calls into question the definition of membrane microviscosity from anisotropy measurements. Combined steady-state anisotropy measurements and differential phase fluorometry more accurately describe the rotational motions of probes in lipid bilayers and provide a better understanding of the constraints imposed by an anisotropic lipid bilayer. By such experiments it should also be possible to select fluorescence probes whose rotational motions in lipid bilayers are similar to those in homogeneous solutions, and thereby provide a better method for estimating membrane microviscosities.

J. R. LAKOWICZ
Freshwater Biological Institute and
Department of Biochemistry, University of Minnesota, Navarre 55392
F. G. PRENDERGAST
Department of Pharmacology, Mayo Medical School, Rochester, Minnesota 55901

References and Notes

1. M. Shinitzky, A. C. Dianoux, C. Gilter, G. Weber, *Biochemistry* **10**, 2106 (1971).
2. U. Cogan, M. Shinitzky, G. Weber, T. Nishida, *ibid.* **12**, 521 (1973).
3. C. L. Brashford, C. G. Morgan, G. K. Radda, *Biochim. Biophys. Acta* **426**, 157 (1976).
4. K. Jacobson and D. Wobschhall, *Chem. Phys. Lipids* **12**, 117 (1974).
5. N. F. Moore, Y. Barenholz, R. R. Wagner, *J. Virol.* **19**, 126 (1976).
6. M. Shinitzky and M. Inbar, *J. Mol. Biol.* **85**, 603 (1974).
7. M. Shinitzky and Y. Barenholz, *J. Biol. Chem.* **249**, 2652 (1974).
8. B. R. Lentz, Y. Barenholz, T. E. Thompson, *Biochemistry* **15**, 4521 (1976).
9. ———, *ibid.*, p. 4529.
10. L. A. Chen, R. E. Dale, S. Roth, L. Brand, *J. Biol. Chem.* **252**, 2163 (1977).
11. G. Weber, *J. Chem. Phys.* **66**, 4081 (1977).
12. W. W. Mantulin and G. Weber, *ibid.*, p. 4091.
13. Fluorescence polarization (P) and anisotropy (r) may be interconverted by using $P = 3r/(2 + r)$. Fluorescence anisotropy is defined by
$$r = \frac{I_\parallel - I_\parallel}{I_\parallel + 2I_\perp}$$
where $I_\parallel$ and $I_\perp$ are the time-averaged values of $I_\parallel(t)$ and $I_\perp(t)$. The limiting anisotropy r_∞ is related to the average angle (ϕ) to which torsional motions are restricted at times long compared to the fluorescence lifetime by $r_0/r_\infty = 2/(3\cos^2\phi - 1)$. It is important to recognize that r_∞ is a measure of the average angle, and not a measure of the maximum angle through which the fluorophore rotates.
14. J. R. Lakowicz and F. G. Prendergast, unpublished observations.
15. G. Weber, *Acta Phys. Pol.*, in press.
16. R. D. Spencer and G. Weber, *Ann. N.Y. Acad. Sci.* **158**, 361 (1969).
17. ———, *J. Chem. Phys.* **52**, 1654 (1970).
18. We thank the Freshwater Biological Research Foundation, and especially its founder, R. Gray, Sr., without whose assistance this work would not have been possible. We also thank D. Hogen for valuable technical assistance. The generous support of the American Heart Association, the Mayo Foundation, and the National Institutes of Health under grants ES GM 01238-01A1 (to J.R.L.) and CA 150 83-00 (to F.G.P.) is acknowledged. J.R.L. is an established investigator of the American Heart Association. Our special thanks are due to G. Weber for having supplied us with the theory of hindered rotations (as yet unpublished), and for his continuous generous support of this work.

8 November 1977; revised 18 January 1978

Comparison of Rhapidosomes and Asbestos Microfibrils

Abstract. *Rhapidosomes (cylindrical nucleoprotein rods of bacterial origin) show great structural similarity to the microfibrils of chrysotile asbestos when negatively stained and observed with the electron microscope. If the negative stain is omitted, the asbestos retains its structural detail whereas the rhapidosomes appear to be unstructured bodies. When the microscope is adjusted into a selected area diffraction mode, the asbestos shows characteristic electron diffraction patterns whereas the rhapidosomes appear to be amorphous to electron diffraction.*

Rhapidosomes were first described by Lewin (*1*) who noted that they appeared to be hollow rods roughly 200 by 30 nm. Subsequent workers have identified rhapidosomes in at least 12 different species of bacteria. Although their origin is still obscure, their biochemical structure has suggested that they may arise from cell membranes as the bacteria undergo lysis (*2*). Correll and Lewin (*3*) have emphasized the remarkable similarity of the physical and chemical properties of rhapidosomes to those of tobacco mosaic virus. We describe here observations on the similarity of rhapidosomes to the microfibrils of chrysotile asbestos and suggest methods whereby the two may be distinguished.

While studying bacterial ultrastructure, we observed numerous rod-shaped bodies on the grid surface separate from the bacterial sections. They were cylindrical in shape and had a central core which in some instances protruded from the main body of the rod, characteristics common to rhapidosomes. Although these rods had somewhat larger diameters than many of the reported rhapido-

0036-8075/78/0623-1401$00.50/0

somes, they were well within the range of diameters when all those reported in the literature were considered.

Since rhapidosomes may be products of bacterial lysis, we examined aged cultures before and after sonication. However, no increase in numbers of the rod-shaped bodies was observed over those in preparations from young cultures.

A consistent observation throughout this work was the great fluctuation in the numbers of rod-shaped bodies from preparations made at different times, even from preparations made at the same time from a single liquid bacterial culture that had been thoroughly agitated on a rotary shaker. This result suggested that at least some of the rod-shaped bodies might have been from a source other than the bacterial cells.

When a bacterial culture was subjected to filtration through Millipore filters of successively decreasing pore size, the filtrate secured from the filter of smallest pore size revealed as many of the large rods as the original suspension. This left no doubt that we were dealing, at least in part, with a contaminating substance on the surface of the grids; further study confirmed our suspicion that the particles resembled the microfibrils of chrysotile asbestos. It seems possible that some of the rod-shaped bodies previously described as rhapidosomes could be chrysotile asbestos.

Improper focusing of the image in the electron microscope can present a clear but greatly distorted image of an asbestos fiber (Fig. 1, a and b). The apparently solid center which results from overfocus closely corresponds to the image of a negatively stained rhapidosome with what has often been described as a stain-filled central core. However, central cores may not always be apparent in electron micrographs, particularly of chrysotile, and so are of very limited diagnostic value.

One obvious source of asbestos became evident when an assistant brought freshly sterilized materials from the autoclave room to the laboratory where grids were normally prepared. He then tossed an asbestos glove onto a bench, and a cloud of dust was seen to arise. A single grid placed in contact with the bench surface where the glove had been dropped revealed over 10^6 rod-shaped bodies of the kind we had originally suspected of being rhapidosomes. A control grid prepared in another laboratory revealed only one rod-shaped structure on its entire surface.

Obviously there are many sources of potential contamination by asbestos in the average laboratory: flame shields, flask clamps, beaker tongs, as well as gloves. It is evident that there is a need for a technique or protocol to distinguish unequivocally between asbestos and organic microtubes such as rhapidosomes, particularly when only minute quantities or mixed samples are available. The need is now increased by the concern that has arisen during the past decade over asbestos as a widespread and dangerous pollutant of air and water.

We compared a quantity of known rhapidosomes of *Spirulina* prepared in the biology laboratory of Wellesley College according to the method of Chang and Allen (*4*) with freshly milled asbestos from the Johns-Manville Jeffrey mine in Quebec Province. Comparative sizes of rhapidosomes and asbestos were first considered. Since the recorded lengths of both asbestos and rhapidosomes show such great variability, it would appear that the outer diameter of the fibers is the critical measurement, if indeed size can be regarded as a diagnostic criterion. From the literature one finds for rhapidosomes a diameter range of 19.5 to 33 nm. In a survey of several hundred chrysotile fibrils from different parts of the world, Yada (*5*) found a range of 10 to 70 nm. The diameter of the known chrysotile asbestos microfibrils examined in the pres-

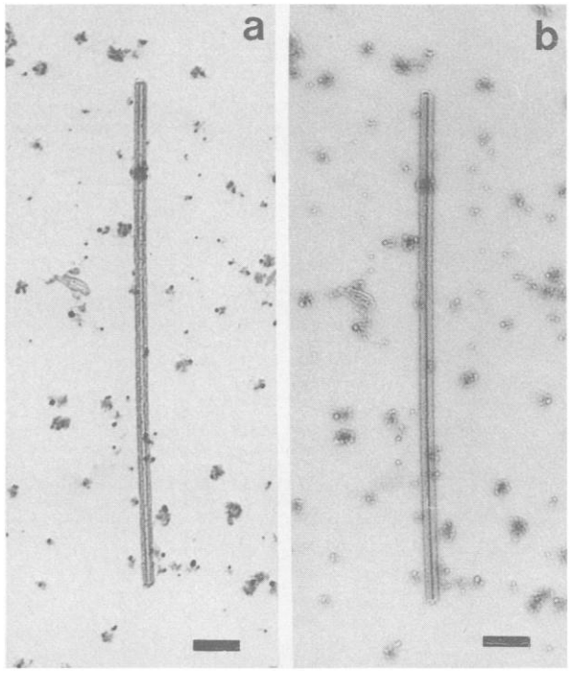

Fig. 1. (a) Microfibril of chrysotile asbestos, negatively stained with 1 percent uranyl acetate, in true focus shows the light core. Scale bar, 100 nm. (b) Same microfibril as that in (a) in overfocus (as indicated by the debris in the background) shows the dark core similar to those of many stained rhapidosomes. Scale bar, 100 nm.

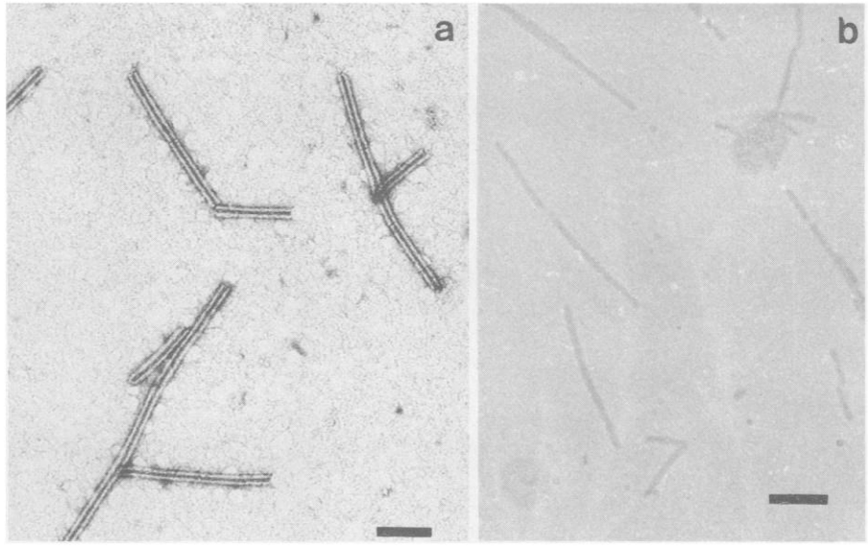

Fig. 2. (a) Rhapidosomes of *Spirulina* negatively stained with 1 percent uranyl acetate. Scale bar, 100 nm. (b) Unstained rhapidosomes of *Spirulina*. Scale bar, 100 nm.

ent study ranged from 23 to 63 nm. Thus, both the rhapidosomes and chrysotile fibrils are within the range of outer diameters (10 to 100 nm) reported in the literature for single fibers of chrysotile from Quebec (*5*, *6*).

Both rhapidosomes and chrysotile also may show telescopic morphology with one tube nesting into another tube (*5*–*7*). However, under high magnification the rhapidosomes occasionally demonstrate a "braided" or spiral appearance. Such braiding has not been observed in chrysotile asbestos, stained or unstained.

In any event it was evident that the similarity of chrysotile asbestos and negatively stained rhapidosomes is too great to permit reliable identifications to be made simply from electron micrographs of negatively stained specimens. Unequivocal results can, however, be obtained rather easily with the use of the standard electron microscope. The technique is based on the fundamental differences in the chemistry and the molecular structures of proteinaceous and silicate fibers. After the samples had been mounted in the usual way on Formvar-coated graphite substrates, micrographs were taken of stained and unstained specimens with an electron microscope (Philips 200). We observed that negative staining with 1 percent uranyl acetate greatly enhanced the rhapidosome images (Fig. 2a). In fact, without such staining the rhapidosomes appeared as completely unstructured bodies (Fig. 2b). However, staining of asbestos microfibrils revealed no increased clarity of the image and no enhancement of structural detail. In fact, a single asbestos microfibril which was studied without staining was reexamined after staining and the two micrographs were indistinguishable. This diagnostically useful result is doubtless due to the low atomic scattering amplitudes of the components of the organic material as compared to those of the chrysotile asbestos [$(OH)_8Mg_6Si_4O_{10}$].

Another diagnostic tool can be applied if the microscope is used for electron diffraction. We found that the chrysotile fibers give their characteristic diffraction patterns (*8*), but that no equivalent patterns could be obtained from the rhapidosomes even at voltages as low as 10 percent of normal.

Confusion is not likely to arise in cases involving types of asbestos other than chrysotile, for example, crocidolite and amosite, which are not tubular. It is conceivable that halloysite [endellite, $(OH)_8Al_4Si_4O_{10} \cdot 4H_2O$], which can have a tubular morphology (*9*) with diameters ranging over those found in rhapidosomes and chrysotile, might, without the techniques discussed in this report, be confused with organic microtubes. However, this mineral does not have the widespread industrial use of asbestos.

W. G. HUTCHINSON
Department of Biology, University of Pennsylvania, Philadelphia 19104
R. IAN HARKER
Department of Geology, University of Pennsylvania
MARY M. ALLEN
Department of Biology, Wellesley College, Wellesley, Massachusetts 02181

References and Notes

1. R. A. Lewin, *Nature (London)* **198**, 103 (1963).
2. J. L. Pate, J. L. Johnson, E. J. Ordal, *J. Cell Biol.* **35**, 15 (1967).
3. D. L. Correll and R. A. Lewin, *Can. J. Microbiol.* **10**, 63 (1964).
4. H. Y. Y. Chang and M. M. Allen, *J. Gen. Microbiol.* **81**, 121 (1974).
5. K. Yada, *Acta Crystallogr. Sect. A* **27**, 659 (1971).
6. T. A. Bates and J. J. Comer, *Proc. 6th Natl. Conf. Clays Clay Minerals* (1959), p. 237; K. Yada, *Acta Crystallogr.* **23**, 704 (1967).
7. J. Chi-Sun Yang, *Am. Mineral.* **46**, 748 (1961); K. Yada and K. Tishi, *J. Cryst. Growth* **24/25**, 627 (1974); *Am. Mineral.* **62**, 958 (1977).
8. J. Zussman, G. W. Brindley, J. J. Comer, *Am Mineral.* **42**, 133 (1957).
9. T. F. Bates *et al.*, *ibid.* **35**, 463 (1950).
10. This work was partially supported by NSF grant DEB-17633 and a Research Corporation Cotrell College science grant to M.M.A.

9 January 1978; revised 7 April 1978

Chemosensory Grazing by Marine Calanoid Copepods (Arthropoda: Crustacea)

Abstract. *In laboratory experiments, mixed populations of two marine copepods* (Acartia clausi *and* Eurytemora herdmani) *when fed artificial food particles consisting of microcapsules that were either enriched with an encapsulated homogenate of naturally occurring phytoplankton or nonenriched preferentially ingested the enriched capsules. Beads or nonenriched capsules were either seldom ingested or not ingested at all. The observations demonstrate that filter-feeding in these species is a behavioral process, under sensory control, and that the copepods are able to discriminate between enriched and nonenriched food particles.*

A number of recent hypotheses concerning the mechanisms of feeding by calanoid copepods suggest that these copepods are able to select particles on the basis of size only and that selection is not behaviorally determined (*1*). It has been claimed that the filtering structure has a variable retention efficiency for natural or artificial particles of different sizes with large particles being more efficiently retained than smaller ones (*1*). By contrast, in other feeding studies performed with naturally occurring particles (*2*) it has been demonstrated that copepods preferentially feed on the sizes of food particles that are most abundant in the

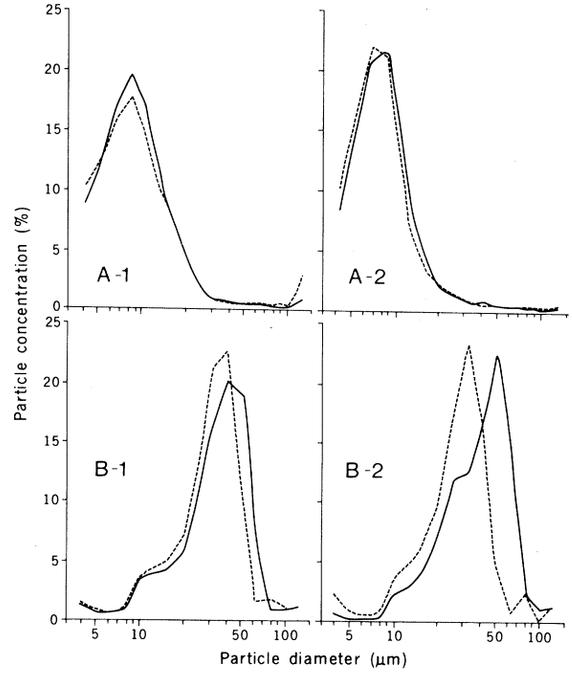

Fig. 1. Feeding activity of copepods measured by comparing unimodal particle size distributions of microcapsules in control (without animals, ——) and in experimental (with animals, ------) bottles. Each curve represents the average of 9 or 15 replicate counts. Experiments A-1 and A-2 were performed, respectively, with small enriched and small nonenriched microcapsules; experiments B-1 and B-2, with large enriched and large nonenriched capsules.

0036-8075/78/0623-1403$00.50/0